MR driven PET-attenuation correction in presence of metal implants using anatomy context driven decisioning

Dattesh D Shanbhag[1], Sandeep S Kaushik[1], Sheshadri Thiruvenkadam[1], Florian Wiesinger[2], Sangtae Ahn[3], Rakesh Mullick[4], and Ravindra M Manjeshwar[5]
[1]*Medical Image Analysis Laboratory, GE Global Research, Bangalore, Karnataka, India,* [2]*Diagnostics & Biomedical Technology Laboratory, GE Global Research, Garching, Bavaria, Germany,* [3]*Functional Imaging Laboratory, GE Global Research, Niskayuna, NY, United States,* [4]*Diagnostics & Biomedical Technologies, GE Global Research, Bangalore, Karnataka, India,* [5]*X-ray & Functional Imaging, GE Global Research, Niskayuna, NY, United States*

Introduction: MR-based PET attenuation correction (AC) is a prerequisite for quantitative PET and key determining factor for the success of PET/MR. Different groups have successfully used different methods to obtain tissue classification for MRAC purpose: intensity based thresholding [1] and active contour/phase field based methods with Dixon images [2] as well as atlas based learning methods [3]. With MRI, tissue segmentation can be confounded due to signal voids in regions of metallic implants **[Figs. 1-4a].** Consequently, metal artifact related areas get mis-classified as air or background in MRAC maps and result in under-estimation of PET uptake [4, 5, 6, 7]. A study based on ~1300 patients has found 10% prevalence of extra-cranial metal (e.g. sutures, stents, chest devices, hip implants) [3]. Therefore, correction of metal implant areas in MRAC map is considered an important unmet need to guarantee accurate and robust MR-based PET-AC [1, 4, 8]. Previously, a semi-automated in-painting method [9] and use of PET contour based method [8] have been proposed to address these issues. Manual in-painting can be cumbersome in clinical workflow. Compared to [8], which uses PET data to achieve closed contour around the body and consequently resolve the artifacts, we demonstrate that this can be achieved with MR data itself using phase field based method [2]. This allows MR and PET processing to be completed simultaneously. Specifically, using a *spatially-adaptive phase field segmentation approach and anatomy context driven decisioning*, we formulated a fully-automatic method to ensure that metal artifacts were either not segmented or if they were, then were removed using the anatomy context. The formulation and results with impact on PET data are demonstrated.

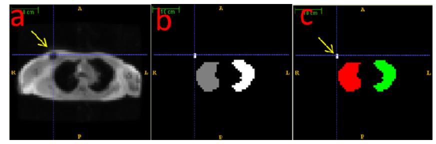

Figure. 1: A representative lung data **(a)** with chemo-port on side (arrow). **(b).** Lung segmentation identified three dark areas **(c).** Lung lobes allow removal of chemo-port artifact

Methods and Materials: PET/MR system: Five patients were selected from a clinical study using an investigational simultaneous PET/MR scanner with TOF capability (GE Healthcare, Waukesha, WI) [7]. The selected cases consisted of those with vertebrae implants, sutures in the surface, chemo-port on the side and water filled lung. **Imaging:** Following standardized injection of 350MBq of FDG and 60min uptake time, imaging started with multi-station, whole-body scanning. MR imaging was performed using a dual-echo spoiled gradient echo sequence (LAVA-Flex) with FA=12°, TE1/TE2/TR=1.15/2.3/4ms, FOV=500x500x312mm^3, matrix=256x256x120pts, 6 bed positions for head to pelvic floor coverage. From the acquired MR data in-phase, out-phase, water and fat images were obtained using DIXON-type reconstruction methods. **MRAC map generation:** The MRAC map consisted of labelling the given Dixon images into: *background, water tissue, fat tissue, internal air and lung*. ***Phase field segmentation method:*** The body contour segmentation as described in [2] generated a smooth, closed contour for the body /background differentiation. For internal air and lung segmentation, compared to [2], the phase field based methodology was made spatially adaptive. Specifically, parameters β (controlling the standard deviation of the background signal distribution and contour smoothness) and λ (capturing the length scale of segmentation) were varied spatially. ***Anatomy partitions and processing***: Following body contour delineation, lung & abdominal stations were partitioned into primary torso, lung lobe, trachea, and vertebrae regions. *Lung Station partitioning:* Two-pass method was adopted. In first pass, spatially invariant lung segmentation [2] was performed with stiff parameters to obtain smooth lung contour and lung lobes identified. Vertebrae region was localized in middle of lung lobes. Second pass of lung segmentation was performed by varying β and λ values in different partition regions. Context information from updated lung lobes was used to eliminate metal artifacts (e.g. chemo-port outside the lung lobes) as well as repainting of missed lung regions due to background incursion. *Abdomen station processing:* For abdomen station, torso extent (excluding the hands on the sides) was identified to enable vertebrae localization in the middle of the torso. The β segmentation parameter was made spatially variant. Metal artifacts in the vertebrae and surrounding regions were removed. **Implementation**: The entire workflow was completely automated and implemented using the functionality available in the Insight Toolkit (ITK) [10]. **PET Reconstruction**: MR-AC maps were generated using fixed AC replacement values: background/air: 0 mm^{-1}, lungs: 0.0018 mm^{-1}, fat: 0.0086 mm^{-1} and water: 0.01 mm^{-1}. PET images were reconstructed by OSEM 2 iterations with post-filtering from both non-TOF and TOF data, using MRAC maps for attenuation correction [11].

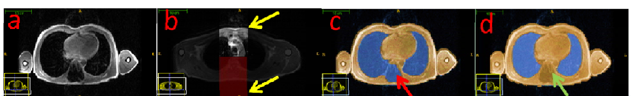

Figure. 2: A representative lung data **(a)** with spinal implant. **(b).** Vertebrae & trachea boxes (arrows). **(c).** lung segmentation using spatially *invariant* parameters, and using **(d)** spatially adaptive method that does not segment vertebrae.

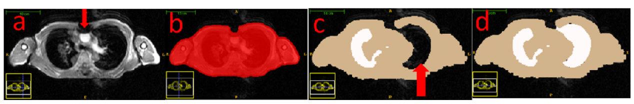

Figure. 3: (a). Lung with surface suture (arrow). **(b).** Phase field based body contour includes surface air **(c)** Removal of surface air results in background incursion and lung is mislabeled. **(d)** Using lung extents information allows repainting.

Result & Discussion: Figures 1, 2 and 3 demonstrate utility of spatially adaptive method in identifying and eliminating metal implant related artifacts in lung station, while reliably segmenting lung. Figure 4 demonstrates the utility of vertebrae region localization to remove spinal implant artifacts in abdomen station and generate a "clean" air mask. Figure 5 demonstrates how these MRAC segmentation changes positively impact the lesion detection in PET, in both non-TOF and TOF PET data. This comparison also demonstrates that TOF mitigate errors due to MR-AC errors [12]. One of the drawbacks of the method was loss of sharp corners of the lungs due to increased smoothness constraints, but can be recovered by additional processing, Secondly, for surface sutures (Fig. 3d), small holes at the surface itself could not be correctly identified as normal tissue (Fig, 3b and d). This can be fixed by detection of abrupt gaps in contour (unpublished work) or PET contour [8].

Conclusion: We have demonstrated that use of spatially and context aware segmentation for MRAC can help address metal implant related issues in segmentation and consequently result in improved fidelity of PET reconstruction. Overall, the presented method will allow for more robust and accurate MR-AC and accordingly PET quantitation in the presence of metallic implants.

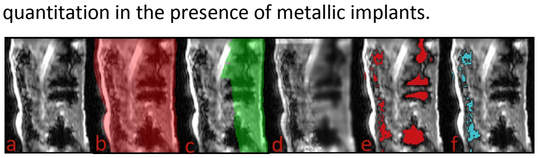

Figure. 4: (a). Abdomen station (sagittal view). **(b).** Torso is reliably identified and **(c).** Allows vertebrae box (green) **(d)** image smoothened in vertebrae region **(e).** Minimizes implant segmentation (f). Processing allows for removal of these metal implant artifacts, while retaining the air pixels.

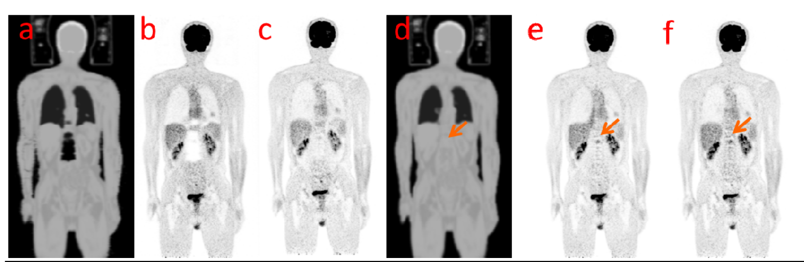

Figure. 5: (a) A whole body MRAC map of a case with spinal implants **(b).** Non-TOF PET recon is severely affected by metal artifacts in MRAC **(c)** and TOF recon is to certain extent by the metal implant artifact in MRAC map, **(d)** the MRAC map post adaptive segmentation. Reliable detection of lesion in PET data (arrows) in both **(e)** non-TOF **(f)** TOF PET reconstructions

References: **[1].** J Nucl Med 2009; 50:520–526 **[2].** IEEE TRANSACTIONS ON NUCLEAR SCIENCE, VOL. 60(5), 2013 **[3].** J Nucl Med. 2008, 49:1875–1883 **[4].** JNM 53: 1415-1426 **[5].** "Philips Ingenuity TF PET/MR attenuation correction", Philips Healthcare **[6].** Med. Phys. 38 (11) 2011 **[7].** MRMPBM, p1-9, 2012 **[8]** Phys. Med. Biol. 59 (2014) 2713–2726 **[9].** Eur J Nucl Med Mol Imag . DOI 10.1007/s00259-012-2316-4 **[10].** www.itk.org **[11].** IEEE Trans.Med. Img. vol. 13, pp. 601-609:1994 **[12].** Conti, Maurizio. Phys. Med. Biol. 56((2011): 155.